Biochimica et Biophysica Acta 1788 (2009) 1271–1278

Contents lists available at ScienceDirect

Biochimica et Biophysica Acta

journal homepage: www.elsevier.com/locate/bbamem

Lipid bilayer disruption by oligomeric α-synuclein depends on bilayer charge and accessibility of the hydrophobic core

Bart D. van Rooijen, Mireille M.A.E. Claessens, Vinod Subramaniam *

Biophysical Engineering Group, MESA+ Institute for Nanotechnology, Faculty of Science and Technology, University of Twente, PO Box 217, 7500 AE, Enschede, The Netherlands

ARTICLE INFO

Article history:
Received 21 November 2008
Received in revised form 27 February 2009
Accepted 13 March 2009
Available online 27 March 2009

Keywords:
Amyloid
Synuclein
Lipid interaction
Pore
Membrane

ABSTRACT

Soluble oligomeric aggregates of α-synuclein have been implicated to play a central role in the pathogenesis of Parkinson's disease. Disruption and permeabilization of lipid bilayers by α-synuclein oligomers is postulated as a toxic mechanism, but the molecular details controlling the oligomer–membrane interaction are still unknown. Here we show that membrane disruption strongly depends on the accessibility of the hydrophobic membrane core and that charge interactions play an important but complex role. We systematically studied the influence of the physical membrane properties and solution conditions on lipid bilayer disruption by oligomers using a dye release assay. Varying the lipid headgroup composition revealed that membrane disruption only occurs for negatively charged bilayers. Furthermore, the electrostatic repulsion between the negatively charged α-synuclein and the negative surface charge of the bilayer inhibits vesicle disruption at low ionic strength. The disruption of negatively charged vesicles further depends on lipid packing parameters. Bilayer composition changes that result in an increased lipid headgroup spacing make vesicles more prone to disruption, suggesting that the accessibility of the bilayer hydrocarbon core modulates oligomer–membrane interaction. These data shed important new insights into the driving forces governing the highly debated process of oligomer–membrane interactions.

1. Introduction

Parkinson's disease (PD) is a common neurodegenerative disorder marked by increased cell death within the substantia nigra [1]. The molecular mechanisms causing this neuronal cell loss remain a mystery, hampering the development of an effective treatment for the disease. The pathological hallmark of PD is the occurrence of intracellular deposits of aggregated protein within Lewy bodies and Lewy neurites [2]. These inclusion bodies contain a large amount of the protein α-synuclein (αS), which suggests that this protein might be involved in the pathogenesis of the disease [3]. Three point mutations of αS causing rare early-onset forms of the disease have been identified [4–6]. Additionally, αS gene duplication [7] and triplication [8] have been linked to PD and diffuse Lewy body disease.

αS is a 140 amino acid protein which is expressed throughout the whole human central nervous system [9]. Although its exact role within the cell is unknown it has been suggested that membrane interaction is important for its function [10]. In aqueous solution αS adopts a random coil conformation [11], but in the presence of negatively charged phospholipid vesicles, the N-terminal residues ~1–100 have been shown to facilitate lipid binding by adopting an α-helical conformation [12–15]. In vitro, αS can aggregate into amyloid-like fibrils rich in β-sheet structure that resemble those found in neuronal protein deposits *in vivo* [16].

Although Lewy bodies have historically been associated with Parkinsonism, their role in the onset and progression of the disease is not understood [17–19]. The amount of fibrillar aggregates within the brain does not necessarily correlate with disease progression [20]. Furthermore, familial disease mutants exhibit larger oligomerization rates, but not enhanced fibril formation [21]. As a result, early oligomeric intermediates in the aggregation process of αS have been hypothesized to be the toxic species. A proposed mechanism of toxicity is lipid membrane disruption [22,23]. An increased permeability of the cellular membrane could lead to neurodegeneration via an altered calcium homeostasis [24]. In vitro it has been shown that αS spherical oligomers can disrupt phospholipid vesicles [25]. The proposed disruption mechanism is the formation of pore-like structures within the lipid bilayer. This hypothesis has been supported by single channel recording [26,27], a selectivity for the marker size in an efflux assay [28] and the observation of donut shaped complexes by atomic force microcopy and electron microscopy [29,30].

The pore-like mechanism is still highly controversial and other mechanisms such as bilayer thinning have been proposed [31]. To correctly identify the mechanism through which membrane permeabilization is facilitated, it is crucial to understand the interaction between the oligomers and lipids. However, very little is known about what factors determine this interaction.

* Corresponding author. Fax: +31 53 4891105.
E-mail address: V.Subramaniam@utwente.nl (V. Subramaniam).

0005-2736/$ – see front matter © 2009 Elsevier B.V. All rights reserved.
doi:10.1016/j.bbamem.2009.03.010

To address this issue we comprehensively studied the membrane disruptive effect of αS oligomers using a dye release assay on lipid vesicles. By systematically altering the vesicle lipid composition and solution conditions we mapped the fundamental driving forces governing the oligomer–lipid interaction. We show that membrane permeabilization is mainly determined by the presence of negatively charged lipids in the bilayer. At low ionic strengths, vesicle disruption was inhibited, thereby suggesting a complex role for electrostatic interactions. Furthermore, both the headgroup specificity of the interaction and the dependence on the bilayer packing parameters imply that disruption occurs through interaction with the bilayer core.

2. Materials and methods

2.1. Expression and purification of recombinant αS

Expression of the human wild-type αS and the disease related mutant proteins A30P, E46K and A53T were performed as described [32].

2.2. Preparation of αS oligomeric and fibrillar species

To prepare the αS oligomeric species, 250 μM stock solutions of αS monomers in 10 mM Hepes pH 7.4, were dried in a vacuum evaporator and dissolved using MilliQ water at a protein concentration of 1 mM. The protein solution was incubated in an Eppendorf thermo mixer for 18 h at room temperature at 1250 rpm. After filtration through a 0.2 μm spin-X centrifugal filter (Corning) to remove possible large aggregates, the oligomeric species were separated from the monomeric protein by size-exclusion chromatography on a Superdex 200 (GE) gel filtration column using 10 mM Hepes pH 7.4, 150 mM NaCl as eluant. Fractions containing the αS oligomers, judged from UV absorption spectra, were pooled and concentrated using a Vivaspin (Sartorius) concentrator with a 10 kDa molecular weight cutoff. The protein concentration was estimated by measuring the absorption at 275 nm. A correction for scattering was applied as [33], which was generally around 10–15% in magnitude. Mature αS fibrils were prepared by incubating the stock protein solution in a thermo mixer for 10 days at 37 °C at 1250 rpm. The aggregated protein was pelleted by centrifugation for 40 min at 21,000 × g. The pellet was washed and resuspended twice in 10 mM Hepes, pH 7.4, 150 mM NaCl. To estimate the protein concentration in the fibril containing solution, the aggregates were dissolved in 5M guanidine hydrochloride, and the protein concentration was calculated from the absorption measured at 275 nm.

2.3. Immunoblotting

2 μl of monomeric and oligomeric αS (20 μM both) were absorbed to a nitrocellulose membrane. After blocking for 2 h with 10% non fat dry milk, 10 mM Tris–HCl pH7.4, 150 mM NaCl, 0.05% Tween20, dot blots were incubated for 2 h with either the A11 anti oligomeric antibody (Chemicon) or an anti αS antibody (Sigma) in 5% non fat dry milk, 10 mM Tris–HCl pH7.4, 150 mM NaCl, 0.05% Tween20. Subsequently blots were incubated for 1 h with a goat-anti-mouse secondary antibody coupled to horse radish peroxide (Sigma). Immunoreactivity was detected on a Nikon imaging station from the luminescence after adding SuperSignal pico substrate (Pierce).

2.4. Native gradient PAGE

Polyacrylamide gels were cast with a linear gradient from 3 to 17%. Gels were run under non-denaturing conditions. Ferritin (440 kDa) was loaded as a molecular weight marker.

2.5. Atomic force microscopy

Atomic force microscopy (AFM) images were obtained using tapping mode AFM in air, on custom-built equipment [34]. Samples were prepared by placing a 5 μl drop of protein solution on a piece of freshly cleaved mica. The protein was allowed to adsorb to the surface by incubating for 5 min in a humid environment. After incubation, excess liquid was removed and the sample was washed twice with 20 μl MilliQ water which was immediately blotted off. Finally, the sample was dried under a gentle stream of nitrogen gas.

2.6. Electron microscopy

A 5 μl aliquot of protein solution was placed on a carbon coated copper grid and was allowed to adsorb to the grid during a 5 minute incubation period under a humid atmosphere to prevent complete drying. Drops of MilliQ water and 2% ammonium molybdate were placed on a piece of parafilm. The grid was washed by touching the drop of MilliQ water which was immediately blotted off. The grid was then stained by touching a drop of staining solution which was blotted off after 30 s. The samples were imaged in a Philips CM300ST-FEG transmission electron microscope.

2.7. Circular dichroism

Circular dichroism (CD) spectra were recorded using a Jasco 715 spectropolarimeter using a 0.05 cm path length quartz cuvette. Monomeric and oligomeric species of αS at 10 μM concentration were prepared in 5 mM Tris–Borate pH 7.5 buffer. After recording the CD spectra, POPG LUVs obtained by extrusion through an 80 nm filter were added to a final protein lipid ratio of 1:100 and the spectrum in the presence of lipids was recorded.

2.8. Liposome preparation

1-Palmitoyl, 2-oleoyl phosphatidylcholine (POPC), 1-palmitoyl, 2-oleoyl phosphatidylglycerol (POPG), 1,2-dioleoyl phosphatidylglycerol (DOPG), 1-oleoyl phosphatidylglycerol (lyso PG), 1,2-dilinoleoyl phosphatidylglycerol (18:2 PG), 1-palmitoyl, 2-oleoyl phosphatidylserine (POPS), 1,2-dioleoyl phosphatidylserine (DOPS), 1,2-dioleoyl phosphatidic acid (DOPA), 1,2-dioleoyl phosphatidylethanolamine (DOPE), soy L-α-phosphatidylinositol (PI), bovine heart cardiolipin (CL) and cholesterol (chol) were all obtained from Avanti Polar lipids and used without further purification. The various lipid compositions were prepared by mixing the chloroform dissolved lipids to specific ratios. Lipid acyl chain compositions were chosen to minimize the chance of phase separation in the mixtures. To prepare large unilamellar vesicles (LUVs), a thin lipid film was formed by drying around 0.5 mg of lipid in a glass tube using a gentle stream of N2. Trace amounts of solvent were removed by drying under vacuum for 4 h. The lipid film was then hydrated by adding a solution of 50 mM calcein (Sigma), 10 mM Hepes, pH 7.4 Appropriate amounts of NaCl were added to maintain an osmotic strength equal to 10 mM Hepes pH 7.4, 150 mM NaCl. Hydration was continued for 1 h, with vortexing approximately every 15 min. The sample was subsequently subjected to 5 freeze–thaw cycles by dipping into liquid nitrogen and thawing above the lipid phase transition temperature. The resulting solution was extruded 11 times through a polycarbonate membrane filter with a defined pore size. This procedure was repeated once with a new filter. Unencapsulated dye was separated from the vesicles by gel filtration through a PD10 column packed with Sephadex G-100 (GE). The vesicle size distribution was measured using dynamic light scattering on a Malvern Zetasizer 4000 instrument. The total phospholipid concentration was determined according to the protocol of Chen et al. [35].

2.9. Efflux assay

For the efflux assay the stock vesicle solution was first diluted to twice the final phospholipid concentration and then thoroughly mixed with an equal volume of protein solution. After 30 minutes of incubation the maximum intensity of the fluorescence emission spectrum for excitation at 497 nm was recorded on a Varian Cary Eclipse fluorimeter. After subtraction of the background, leakage was expressed as a percentage of the maximum possible effect due to vesicle disruption induced by the addition of 0.5% (weight/volume) Triton X-100. All experiments were performed in triplicate. The standard deviations from these triplicates are indicated as the error bars in all figures. Experiments aiming to elucidate the influence of a certain single parameter were performed on the same preparation of oligomers, to negate possible batch to batch differences in oligomer preparation and potential errors in the concentration determination.

2.10. Ionic strength assay

For the ionic strength experiment, solutions of 10 mM Hepes pH 7.4 containing 0 mM, 5 mM or 50 mM NaCl were prepared. For these solutions vesicles were hydrated in 50 mM calcein, 10 mM Hepes pH 7.4. The NaCl buffer solutions were adjusted with sucrose to equal osmolarity as the vesicle hydration solution. Vesicles for the NaCl concentration of 150 mM were prepared as described earlier. αS oligomers were prepared in the appropriate buffer by buffer exchange from a stock solution, using a Zeba Spin desalting column (Pierce).

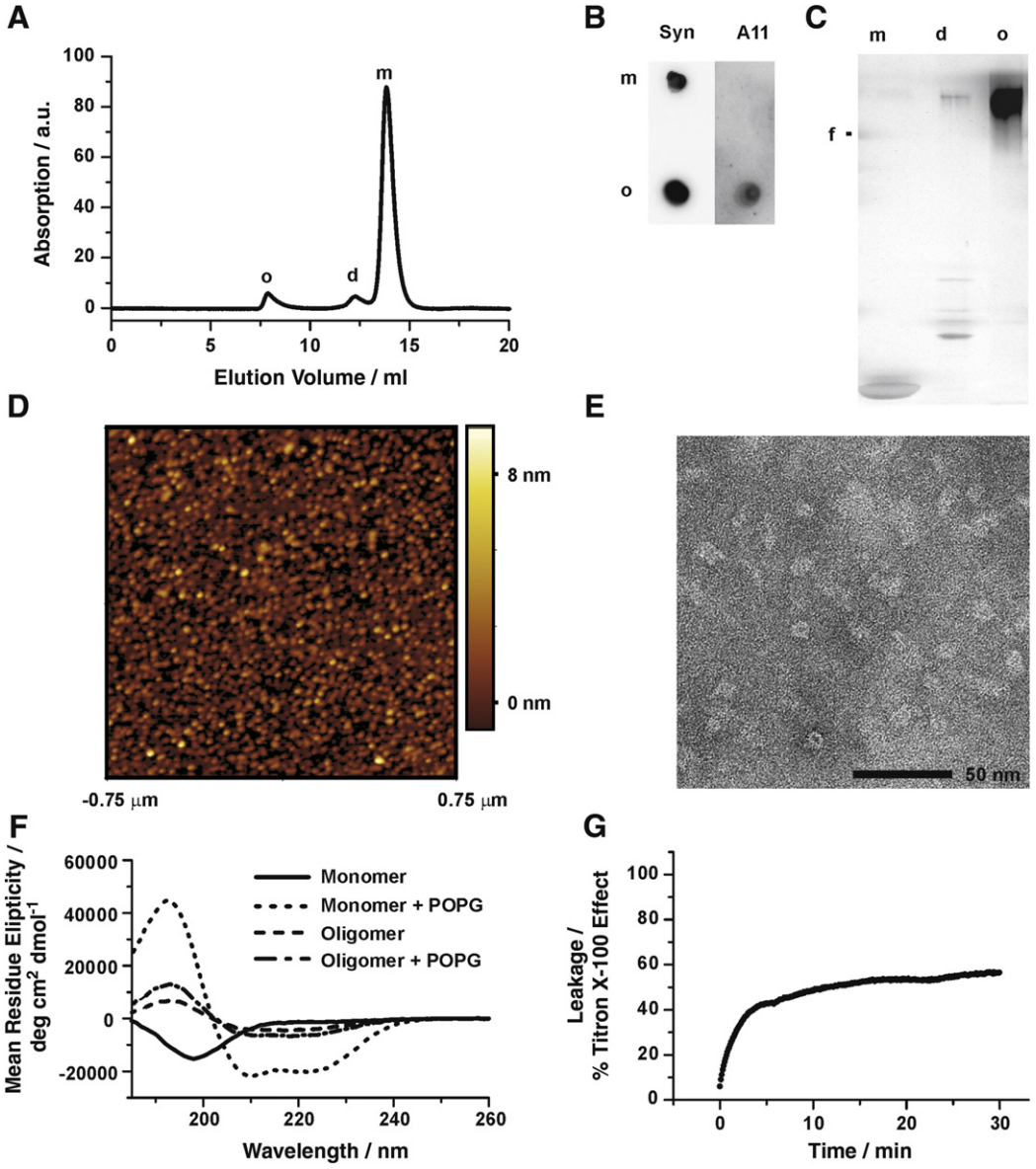

Fig. 1. Characterization of purified oligomeric wild type αS. (A) Size exclusion chromatogram of the purification of αS oligomers. The oligomeric peak (o) is easily separated from the monomeric (m) peak. Smaller aggregates, possibly dimers (d), elute just before the monomeric peak. (B) Immunoblotting with anti αS and the A11 anti oligomeric antibody. Anti αS antibody showed both reactivity to monomeric (m) and oligomeric (o) αS. The anti oligomeric αS antibody only showed reactivity to oligomeric αS. (C) Native gradient PAGE with a polyacrylamide gradient form 3 to 17%. Purified αS oligomers did not contain any monomeric protein. Lanes were loaded with fractions from the oligomeric (o), dimeric (d) and monomeric (m) peak of the chromatogram shown in A. Ferritin (f) was included as a molecular weight marker (440 kDa). Oligomeric αS is observed as a broad high molecular weight band above the ferritin band. (D) Tapping mode AFM in air of αS oligomers adsorbed to a mica surface (1.5 μm scan size). (E) TEM image of ammonium molybdate stained oligomers. (F) CD spectrum of monomeric and oligomeric αS in the presence and absence of POPG LUVs. (G) Kinetics of calcein efflux from 20 μM POPG LUVs as induced by 0.015 μM oligomeric αS. The leakage kinetics contains an initial fast phase, after which leakage gradually continues.

3. Results

3.1. Oligomer characterization

One of the challenges in elucidating the interaction between αS oligomers and phospholipids is reliable production of the oligomeric species. Little is known about the actual structure of the oligomeric intermediate and its role in the aggregation process. Purification of the oligomers generally does not result in a single homogenous population of an oligomeric state but rather gives a broad distribution of protein aggregates of different sizes [29]. We therefore carefully characterized the oligomeric species produced.

Preparation of oligomeric αS resulted in low yields (2–4%), as can be seen in the chromatogram in Fig. 1A. Increasing the incubation time did not improve the yield, possibly due to the consumption of these oligomers by fibrillar αS. The purified oligomers bound the A11 antibody, which is specific for oligomeric intermediates in the aggregation pathway of many amyloidogenic proteins [36] (Fig. 1B). No monomeric αS could be detected in the purified oligomer solutions using native PAGE (Fig. 1C).

In AFM images the purified oligomers appeared as spherical aggregates with heights in the range of 2–8 nm (Fig. 1D). Electron microscopy images of negatively stained oligomers showed spherical and donut shaped particles of around 6–11 nm (Fig. 1E).

The secondary structure of the oligomeric species was characterized using CD spectroscopy. The oligomeric intermediate has been reported to possess a β-sheet structure [25]. Monomeric αS showed a CD spectrum characteristic of an intrinsically disordered protein (Fig. 1F). Addition of an excess of negatively charged POPG lipid vesicles induced a conformational change to a predominantly α-helical structure as has been reported before [13]. The purified oligomeric species contained β-sheet structure, and no major conformational changes were observed upon the addition of anionic lipids.

3.2. Membrane permeabilization

Membrane disruption by αS was characterized using a dye efflux assay. LUVs were filled with 50 mM calcein, a concentration at which calcein fluorescence self-quenches. Upon leakage from the vesicle, quenching of the dye is relieved and a fluorescence signal is observed. The intensity after 30 min of incubation was measured. The kinetics of dye leakage induced by oligomeric αS are relatively fast, making this essentially an endpoint measurement (Fig. 1G). The extent of dye leakage from POPG LUVs was clearly dependent on the protein concentration for all aggregation states (Fig. 2). Oligomeric αS was the most effective in disrupting the LUVs and induced a 50% leakage of the LUVs at a concentration of ~0.13 μM. Both the monomeric and fibrillar form of the protein were also able to disrupt the LUVs, although at significantly higher protein concentrations. These induced 50% vesicle leakage at ~21 μM and ~7.0 μM respectively. The disease related mutants A30P, E46K and A53T showed similar disruptive properties (Fig. 3).

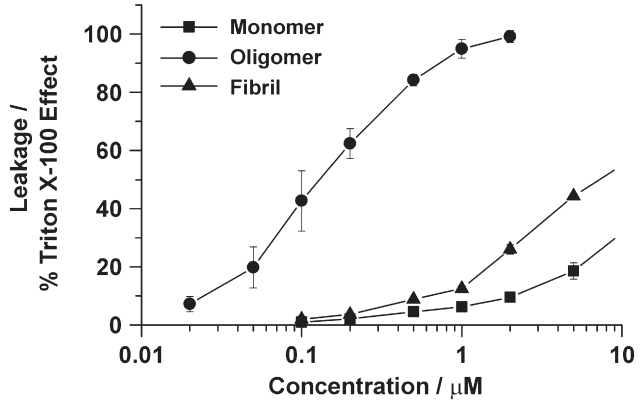

Fig. 2. Dependence of the content leakage from POPG LUVs on the concentration of αS monomers, oligomers and fibrils at a phospholipid concentration of 20 μM. Leakage is expressed as a percentage of the maximum possible effect induced by the addition of Triton X-100. The protein concentration for the oligomeric and fibrillar species is given as the equivalent monomer concentration.

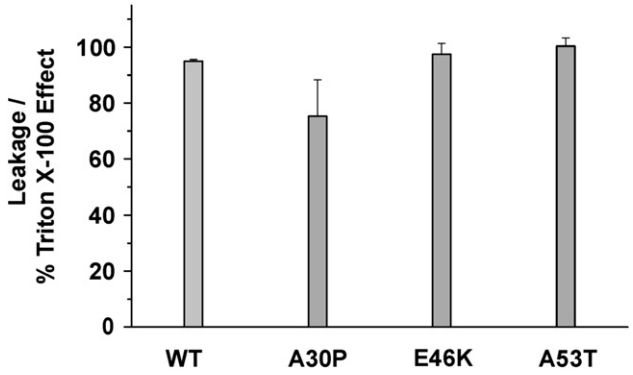

Fig. 3. Calcein efflux from 20 μM POPG LUVs induced by 1 μM oligomeric αS (grey bars) from wild type (WT), A30P, E46K and A53T αS. Oligomers from all mutants were able to disrupt the POPG LUVs.

3.3. Lipid headgroup specificity

It is not known which properties of the lipid bilayer determine the interaction with the oligomeric intermediates. Membrane permeabilization by αS oligomers has been reported to depend on lipid headgroup composition [28,37], but the data are contradictory. To assess the headgroup specificity for membrane disruption, we prepared LUVs composed of phospholipids with different headgroups. The results from these experiments clearly show that only vesicles composed of negatively charged phospholipids show dye efflux upon addition of 1 μM of oligomeric αS (Fig. 4). POPG, PI and DOPS all showed calcein efflux upon addition of the oligomeric species. LUVs from the zwitterionic POPC were not disrupted by αS. This suggests that charge interactions play an important role in oligomer–lipid interaction. Mixing zwitterionic lipids, such as POPC and DOPE, with anionic lipids in a 1:1 molar ratio, inhibited the vesicle disruption for POPG, DOPS and PI containing vesicles. Vesicle preparations from the anionic lipids DOPA and CL were rather unstable. Therefore, to probe the interaction of oligomeric αS with these lipids, vesicles were prepared from 1:1 mixtures of anionic CL and DOPA with zwitterionic POPC. These vesicles showed considerable dye release. When the ratio of zwitterionic lipids to anionic lipid was changed to 3:1, dye efflux was fully inhibited in both the POPC:DOPA and the POPC:CL LUVs.

Monomeric and fibrillar αS were also added to the LUVs at a ten times higher concentration. These induced some dye efflux from POPG LUVs and from PI LUVs. The amount of efflux was still smaller than the efflux induced by 1 μM oligomeric αS.

To further investigate the role of charge interactions in αS induced membrane disruption, a dye release experiment at different ionic strengths was performed (Fig. 5). This revealed very clearly that at low ionic strength (0 and 5 mM added NaCl) vesicle disruption was strongly inhibited. At higher salt concentrations of 50 mM and 150 mM NaCl a clear concentration dependent calcein efflux was observed.

3.4. Lipid packing parameters

The increased sensitivity of DOPA and CL to oligomeric αS might be related to their small headgroup size. Thus the accessibility of the

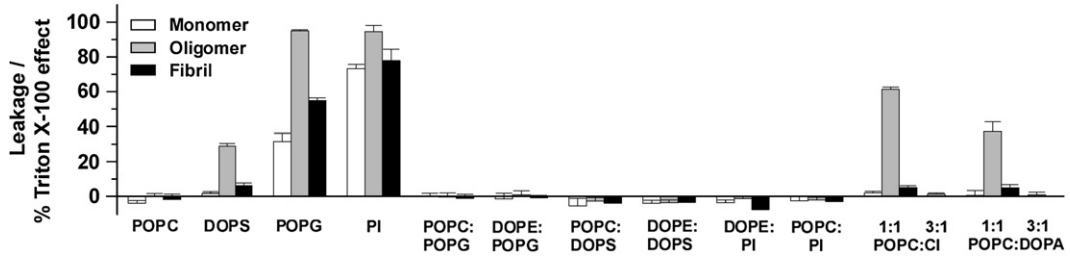

Fig. 4. Calcein efflux from LUVs of different lipid compositions induced by 10 μM monomeric, 1 μM oligomeric and 10 μM fibrillar at a phospholipid concentration of 20 μM. Lipid mixtures were prepared in a 1:1 molar ratio, unless noted otherwise.

hydrocarbon bilayer core could be important in determining the lipid interaction of oligomeric αS. Moreover, small unilamellar vesicles (~30 nm) have been shown to be more vulnerable to disruption by the oligomeric species [25]. Curvature stress within the bilayer, which can lead to packing defects, is a possible explanation for such an effect. Although the exact nature of such defects is not clear, they might allow proteins to more easily interact with the hydrophobic core of the membrane [38]. These data indicate that lipid packing parameters could critically determine oligomer–lipid interactions. We therefore investigated the effect of lipid packing properties on the disruption of vesicles by αS oligomers.

First, lipid packing was modulated by altering the spontaneous curvature of the phospholipids in the bilayer which is known to have a large effect on lipid protein interaction [38,39]. The spontaneous curvature of a lipid monolayer is a result of the shape of the lipids [40]. Lipids with a small headgroup have a negative radius of curvature, whereas lipids with a single acyl chain have a positive radius of curvature [38]. DOPA, CL and POPG in high salt concentrations are expected to have negative spontaneous curvature [41]. However in LUVs the lipids are packed in an almost planar bilayer. Thus in vesicles composed of these lipids the hydrophobic lipid bilayer core might be more exposed to the oligomers. The spontaneous curvature can be modulated towards a more positive value without changing the headgroup compositions by adding lipids with a single acyl chain [41] thereby optimizing lipid packing of the LUVs and relieving curvature stress. Lyso PG was added at different ratios to POPG from which LUVs were subsequently obtained by extrusion. Membrane permeability induced by the addition of αS oligomers was measured at different protein concentrations. The results are shown in Fig. 6A. Pure POPG LUVs showed a 50% leakage at a αS concentration of 0.25 μM. Optimizing the lipid bilayer packing by the addition of increasing amounts of lyso PG stabilized the vesicles against permeabilization by αS, with 50% leakage at 0.42 μM αS for 10% lyso PG and at 0.79 μM αS for 20% lyso PG containing vesicles. This result indicates that lipid packing of the LUVs, and thus the accessibility of the membrane core, is an important factor in oligomer–lipid interaction.

Lipid packing is also affected by changing the amount of unsaturated bonds in the lipid hydrocarbon chains. Upon increasing unsaturation, chain disorder increases and the average headgroup spacing becomes larger, resulting in a thinner bilayer [42]. To probe the effects of lipid chain packing, LUVs of lipids with phosphatidyl glycerol headgroups containing different acyl chain configurations were produced. Fully saturated lipids were not probed because of the high gel to fluid phase transition temperature of these lipids. Furthermore, POPG LUVs containing 25% cholesterol were prepared.

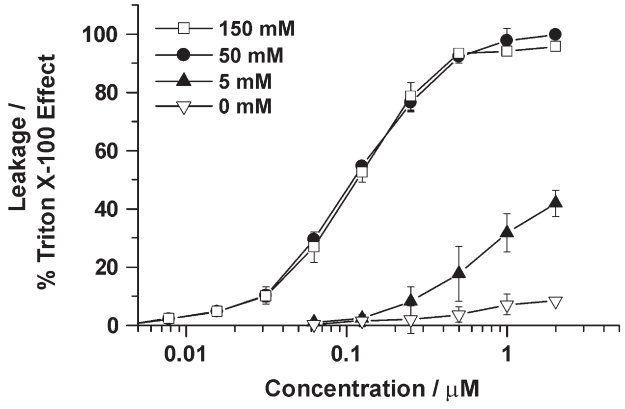

Fig. 5. The effect of the ionic strength of the solution on the disruption of POPG LUVs measured by calcein efflux at a phospholipid concentration of 20 μM. αS oligomers were added at different concentrations to the vesicle solution in the presence of 0 mM, 5 mM, 50 mM and 150 mM NaCl.

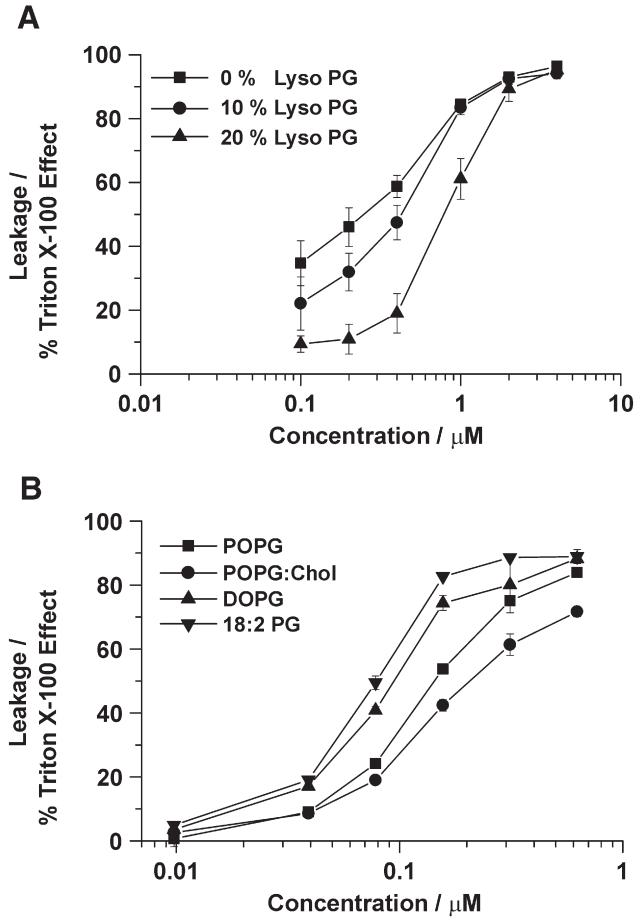

Fig. 6. (A) The effect of headgroup spacing on oligomer-induced vesicle leakage. LUVs were prepared from POPG with different amounts of lyso-PG. Total lipid concentration was 25 μM with vesicles containing 0%, 10% and 20% lyso PG. (B) Influence of lipid packing parameters on oligomer induced vesicle disruption. Plot of the concentration dependent oligomer-induced dye release from 20 μM PG LUVs with different acyl chains: POPG, DOPG, 18:2 PG and POPG:cholesterol 3:1.

Cholesterol is a well known modulator of lipid bilayer packing and enhances the cohesive interactions within the bilayer which results in a more densely packed bilayer [42]. The effect of αS on the permeability of these different LUVs was measured at different oligomer concentrations as shown in Fig. 6B. The results reveal that upon increasing saturation the vesicles are more stable against αS induced permeabilization. The amount of dye release from the different lipid compositions was most efficient in 18:2 PG and decreased upon increasing chain saturation. The addition of 25% cholesterol to POPG LUVs further stabilized these vesicles. The oligomer concentrations at which 50% leakage is induced are as follows: 18:2 PG 0.08 μM, DOPG 0.1 μM, POPG 0.15 μM and POPG:Chol 0.2 μM. These data confirm that an increase in lipid headgroup spacing facilitates the interaction of the oligomer with the membrane.

Interestingly monomeric αS has been reported to optimize lipid packing in small vesicle [43]. Correspondingly, adding a small amount of monomeric αS to LUVs can prevent the membrane permeabilization by oligomeric αS (Supporting information, Fig. S1).

4. Discussion

Membrane disruption by αS oligomers is often considered as a likely mechanism of cytotoxicity in PD. However, due to the lack of understanding of the fundamental molecular mechanisms involved, it is difficult to estimate the biological relevance of this process. In this work we sought to elucidate the fundamental driving forces governing oligomer–lipid interactions by studying how physicochemical bilayer properties influence αS oligomer-induced vesicle disruption.

Oligomeric αS is generally prepared by allowing the protein to aggregate for a certain time and isolating the oligomeric intermediates before they are converted into fibrillar αS. A multitude of conditions have been applied in different laboratories to induce αS oligomerization. These different conditions might result in structurally and functionally different oligomers and can therefore be difficult to compare. The structure of αS is experimentally not easily accessible and no detailed structural information is available. Generally, αS oligomers are reported as spherical protein aggregates with sizes between 2 and 20 nm. Annular and tubular morphologies are sometimes reported. We have used an increased protein concentration to induce aggregation. Oligomeric αS prepared using this protocol exhibit morphological and structural characteristics similar to those reported by others [29,30].

4.1. Vesicle permeabilization

Our experiments clearly show that αS oligomers can permeabilize POPG LUVs in a concentration dependent fashion. Using similar conditions, Volles et al. [28] found leakage at around 30 times lower protein to lipid ratios; this is possibly the result of the size of the markers used in the different assays used: calcein efflux versus calcium influx. Furthermore, the divalent calcium cation can have a profound effect on negatively charged vesicles in general and on αS–lipid interaction specifically [44,45].

At very high protein concentrations monomeric and fibrillar forms of αS were also able to induce calcein leakage from POPG LUVs. Monomeric αS is thought to disrupt LUVs in a detergent like way. How fibrillar αS could cause membrane damage is not known; apparently fibrillar αS is able to bind to a lipid bilayer. We however cannot exclude the possibility that the monomeric protein forms aggregates on the lipid membranes or that the fibrils dissociate into oligomers. Oligomerization of monomeric αS on the membrane surface has been suggested by MD simulation [46] and aggregation experiments [47], while single channel activity has been observed upon addition of the monomeric protein [48].

αS oligomers from the disease related mutants A30P, E46K and A53T showed very similar leakage characteristics. Although no major quantitative difference in induced leakage was observed between the different mutants, oligomers derived from A30P αS appeared to induce the least vesicle disruption. Interestingly, monomeric A30P αS is also reported to bind lipids with a lower affinity than wild type αS and the E46K and A53T mutants [49,50].

4.2. Driving forces

Our results indicate that only negatively charged vesicles are affected by oligomeric αS. Therefore charge interactions appear to determine oligomer mediated membrane disruption. Monomeric αS, although highly negatively charged, specifically binds to negatively charged membranes [13,14]. This binding is explained by the fact that at neutral pH the N-terminal lipid binding region contains many positively charged residues. Furthermore, most of the negative charge is concentrated in the C-terminus of the protein, which remains unstructured in solution upon protein–lipid binding [51]. Although the structure of oligomeric αS in its free and lipid bound state is not known, a clear charge separation as in the monomeric protein seems unlikely to be energetically favorable. However binding of oligomeric αS to negatively charged vesicles has been reported [28] and we have observed a binding specificity of oligomeric αS for negatively charged lipids [52]. Therefore charge interactions appear to play a crucial role in oligomer–lipid binding.

The role of charge interactions in oligomer membrane disruption appears to be more complex. Calcein efflux experiments at different ionic strengths showed that leakage is inhibited at low salt concentrations. For binding mediated by charge interaction we would have expected to observe stronger binding and thus leakage at lower protein concentrations. Possibly, reduced screening of electrostatic interactions at low ionic strength between the negatively charged oligomers and the bilayer surface causes an electrostatic repulsion inhibiting binding. Positively charged or hydrophobic patches on the surface of the oligomer might support the oligomer binding. However, there are many contributing factors making it difficult to pinpoint the exact binding mechanism. For instance, the structure of the αS oligomers might change as an effect of ionic strength. Finally, lipid packing parameters are also influenced by the ionic strength, further contributing to the complexity of the system.

In addition to bilayer charge, lipid packing parameters also influence the oligomer-induced vesicle disruption. We observed that more densely packed bilayers were more resistant to disruption. This suggests that hydrophobic interactions contribute to oligomer–lipid binding. The membrane interior of loosely packed bilayers is much more accessible. Interaction with the membrane hydrocarbon core might facilitate binding and disruption. Interestingly, addition of monomeric αS protects the LUVs from disruption by oligomeric αS. Monomeric αS is known to bind to defects in the lipid bilayer and thus can have a stabilizing effect on small vesicles [43].

4.3. Mechanism of disruption

One of the key questions in oligomer–lipid interactions revolves around the mechanism by which bilayer disruption occurs. The dependence of membrane disruption on the bilayer physical properties can give important information on the most likely mechanism of membrane disruption [53]. Besides a pore-like mechanism [26,28], membrane thinning has been suggested as a possible mode of action [31,54]. Adsorption of the oligomeric intermediates to the surface of the bilayer could cause an increase in the average headgroup spacing and thus have a thinning effect. Bilayer thinning increases the membrane permeability by decreasing the thickness of the hydrophobic barrier. Lipid bilayers that are more easily compressed are expected to show greater membrane permeability. Addition of cholesterol to the bilayer which reduces the compressibility of the bilayer did show a slight inhibitory effect. Our results suggest that a

thinner membrane with increased headgroup spacing facilitates the leakage process. However, thinning of the bilayer may be the cause of oligomer–lipid interaction and not necessarily the effect. Pore formation through oligomer insertion into the bilayer core still offers a possible explanation for all the observed effects.

4.4. Biological significance

From the observed lipid specificity one could predict likely cellular targets for αS oligomer membrane disruption. The plasma membrane is rich in sterols, sphingolipids and phosphatidylcholines [55]. Our data show that POPC and cholesterol both inhibit leakage therefore the plasma membrane is not a likely target for oligomeric αS.

Although αS in its monomeric and aggregated form have been observed in the extracellular space and can be possible secreted or released from dying cells [56], the majority of the protein is intracytoplasmic. Therefore the membranes of organelles are also a possible target of αS oligomers. In this light the observed leakage specificity for the mitochondrial lipid cardiolipin suggests that mitochondria could be vulnerable to αS oligomers. Mitochondrial dysfunction has long been suggested to play a potential role in the pathogenesis of PD [19]. αS has been observed to localize to mitochondria [57], which is increased upon αS overexpression [58] and intracellular acidification [59]. Mitochondrial localization of αS is possibly mediated by cardiolipin since monomeric αS has been reported to bind cardiolipin with high affinity [60] in vitro. Possibly, αS oligomers directly induce mitochondrial membrane damage. Additionally interactions with mitochondrial proteins, such as mitochondrial complex I could also be a source of cell damage [61–63]. However, it should be pointed out that membrane disruption was only observed in membranes which have high anionic lipid content. At physiologically more relevant concentrations, such as POPC:Cl 3:1 membrane disruption was inhibited. How these results translate to the effect of αS oligomers *in vivo* is unclear, since real biological membranes are much more heterogeneous and contain distinct domains that may mediate oligomer–membrane interactions.

Elucidating the toxic species in the aggregation of αS and pinpointing the exact mechanisms involved still remains one of the biggest challenges in the field. The process of αS aggregation is highly dynamic and a multitude of aggregation intermediates possibly possesses different lipid binding properties. Such a complicated and heterogeneous system is difficult to access experimentally in a cellular context. Therefore biophysical and biochemical data as presented here offer important insights into how oligomeric αS could interact with cellular components.

Appendix A. Supplementary data

Supplementary data associated with this article can be found, in the online version, at doi:10.1016/j.bbamem.2009.03.010.

References

[1] H. Braak, E. Ghebremedhin, U. Rub, H. Bratzke, K. Del Tredici, Stages in the development of Parkinson's disease-related pathology, Cell Tissue Res. 318 (2004) 121–134.
[2] F.H. Lewy, in: L.M. (Ed.), Paralysis Agitans, Handbuch der Neurologie, 1912, pp. 920–933.
[3] M.G. Spillantini, M.L. Schmidt, V.M. Lee, J.Q. Trojanowski, R. Jakes, M. Goedert, Alpha-synuclein in Lewy bodies, Nature 388 (1997) 839–840.
[4] R. Krüger, W. Kuhn, T. Müller, D. Woitalla, M. Graeber, S. Kösel, H. Przuntek, J.T. Epplen, L. Schols, O. Riess, Ala30Pro mutation in the gene encoding alpha-synuclein in Parkinson's disease, Nat. Genet. 18 (1998) 106–108.
[5] M.H. Polymeropoulos, C. Lavedan, E. Leroy, S.E. Ide, A. Dehejia, A. Dutra, B. Pike, H. Root, J. Rubenstein, R. Boyer, E.S. Stenroos, S. Chandrasekharappa, A. Athanassiadou, T. Papapetropoulos, W.G. Johnson, A.M. Lazzarini, R.C. Duvoisin, G. Di Iorio, L.I. Golbe, R.L. Nussbaum, Mutation in the alpha-synuclein gene identified in families with Parkinson's disease, Science 276 (1997) 2045–2047.
[6] J.J. Zarranz, J. Alegre, J.C. Gómez-Esteban, E. Lezcano, R. Ros, I. Ampuero, L. Vidal, J. Hoenicka, O. Rodriguez, B. Atarés, V. Llorens, E. Gomez Tortosa, T. del Ser, D.G. Muñoz, J.G. de Yebenes, The new mutation, E46K, of alpha-synuclein causes Parkinson and Lewy body dementia, Ann. Neurol. 55 (2004) 164–173.
[7] M.C. Chartier-Harlin, J. Kachergus, C. Roumier, V. Mouroux, X. Douay, S. Lincoln, C. Levecque, L. Larvor, J. Andrieux, M. Hulihan, N. Waucquier, L. Defebvre, P. Amouyel, M. Farrer, A. Destée, Alpha-synuclein locus duplication as a cause of familial Parkinson's disease, Lancet 364 (2004) 1167–1169.
[8] A.B. Singleton, M. Farrer, J. Johnson, A. Singleton, S. Hague, J. Kachergus, M. Hulihan, T. Peuralinna, A. Dutra, R. Nussbaum, S. Lincoln, A. Crawley, M. Hanson, D. Maraganore, C. Adler, M.R. Cookson, M. Muenter, M. Baptista, D. Miller, J. Blancato, J. Hardy, K. Gwinn-Hardy, alpha-Synuclein locus triplication causes Parkinson's disease, Science 302 (2003) 841.
[9] D.F. Clayton, J.M. George, The synucleins: a family of proteins involved in synaptic function, plasticity, neurodegeneration and disease, Trends Neurosci. 21 (1998) 249–254.
[10] K. Beyer, Mechanistic aspects of Parkinson's disease: alpha-synuclein and the biomembrane, Cell Biochem. Biophys. 47 (2007) 285–299.
[11] P.H. Weinreb, W. Zhen, A.W. Poon, K.A. Conway, P.T. Lansbury Jr., NACP, a protein implicated in Alzheimer's disease and learning, is natively unfolded, Biochemistry 35 (1996) 13709–13715.
[12] R. Bussell Jr., T.F. Ramlall, D. Eliezer, Helix periodicity, topology, and dynamics of membrane-associated alpha-synuclein, Protein Sci. 14 (2005) 862–872.
[13] W.S. Davidson, A. Jonas, D.F. Clayton, J.M. George, Stabilization of alpha-synuclein secondary structure upon binding to synthetic membranes, J. Biol. Chem. 273 (1998) 9443–9449.
[14] E. Jo, J. McLaurin, C.M. Yip, P. St George-Hyslop, P.E. Fraser, alpha-Synuclein membrane interactions and lipid specificity, J. Biol. Chem. 275 (2000) 34328–34334.
[15] M. Stöckl, P. Fischer, E. Wanker, A. Herrmann, Alpha-synuclein selectively binds to anionic phospholipids embedded in liquid-disordered domains, J. Mol. Biol. 375 (2008) 1394–1404.
[16] K.A. Conway, J.D. Harper, P.T. Lansbury Jr., Fibrils formed in vitro from alpha-synuclein and two mutant forms linked to Parkinson's disease are typical amyloid, Biochemistry 39 (2000) 2552–2563.
[17] M.S. Goldberg, P.T. Lansbury Jr., Is there a cause-and-effect relationship between alpha-synuclein fibrillization and Parkinson's disease? Nat. Cell Biol. 2 (2000) E115–E119.
[18] C.W. Shults, Lewy bodies, Proc. Natl. Acad. Sci. U. S. A. 103 (2006) 1661–1668.
[19] M.R. Cookson, M. van der Brug, Cell systems and the toxic mechanism(s) of alpha-synuclein, Exp. Neurol. 209 (2008) 5–11.
[20] L. Parkkinen, T. Kauppinen, T. Pirttilä, J.M. Autere, I. Alafuzoff, Alpha-synuclein pathology does not predict extrapyramidal symptoms or dementia, Ann. Neurol. 57 (2005) 82–91.
[21] K.A. Conway, S.J. Lee, J.C. Rochet, T.T. Ding, R.E. Williamson, P.T. Lansbury Jr., Acceleration of oligomerization, not fibrillization, is a shared property of both alpha-synuclein mutations linked to early-onset Parkinson's disease: implications for pathogenesis and therapy, Proc. Natl. Acad. Sci. U. S. A. 97 (2000) 571–576.
[22] H.A. Lashuel, D. Hartley, B.M. Petre, T. Walz, P.T. Lansbury Jr., Neurodegenerative disease: amyloid pores from pathogenic mutations, Nature 418 (2002) 291.
[23] K. Furukawa, M. Matsuzaki-Kobayashi, T. Hasegawa, A. Kikuchi, N. Sugeno, Y. Itoyama, Y. Wang, P.J. Yao, I. Bushlin, A. Takeda, Plasma membrane ion permeability induced by mutant alpha-synuclein contributes to the degeneration of neural cells, J. Neurochem. 97 (2006) 1071–1077.
[24] M.P. Mattson, Calcium and neurodegeneration, Aging Cell 6 (2007) 337–350.
[25] M.J. Volles, S.J. Lee, J.C. Rochet, M.D. Shtilerman, T.T. Ding, J.C. Kessler, P.T. Lansbury Jr., Vesicle permeabilization by protofibrillar alpha-synuclein: implications for the pathogenesis and treatment of Parkinson's disease, Biochemistry 40 (2001) 7812–7819.
[26] A. Quist, I. Doudevski, H. Lin, R. Azimova, D. Ng, B. Frangione, B. Kagan, J. Ghiso, R. Lal, Amyloid ion channels: a common structural link for protein-misfolding disease, Proc. Natl. Acad. Sci. U. S. A. 102 (2005) 10427–10432.
[27] M. Kostka, T. Högen, K.M. Danzer, J. Levin, M. Habeck, A. Wirth, R. Wagner, C.G. Glabe, S. Finger, U. Heinzelmann, P. Garidel, W. Duan, C.A. Ross, H. Kretzschmar, A. Giese, Single particle characterization of iron-induced pore-forming alpha-synuclein oligomers, J. Biol. Chem. 283 (2008) 10992–11003.
[28] M.J. Volles, P.T. Lansbury Jr., Vesicle permeabilization by protofibrillar alpha-synuclein is sensitive to Parkinson's disease-linked mutations and occurs by a pore-like mechanism, Biochemistry 41 (2002) 4595–4602.
[29] H.A. Lashuel, B.M. Petre, J. Wall, M. Simon, R.J. Nowak, T. Walz, P.T. Lansbury Jr., Alpha-synuclein, especially the Parkinson's disease-associated mutants, forms pore-like annular and tubular protofibrils, J. Mol. Biol. 322 (2002) 1089–1102.
[30] T.T. Ding, S.J. Lee, J.C. Rochet, P.T. Lansbury Jr., Annular alpha-synuclein protofibrils are produced when spherical protofibrils are incubated in solution or bound to brain-derived membranes, Biochemistry 41 (2002) 10209–10217.
[31] R. Kayed, Y. Sokolov, B. Edmonds, T.M. McIntire, S.C. Milton, J.E. Hall, C.G. Glabe, Permeabilization of lipid bilayers is a common conformation-dependent activity of soluble amyloid oligomers in protein misfolding diseases, J. Biol. Chem. 279 (2004) 46363–46366.
[32] M.E. van Raaij, I.M. Segers-Nolten, V. Subramaniam, Quantitative morphological analysis reveals ultrastructural diversity of amyloid fibrils from alpha-synuclein mutants, Biophys. J. 91 (2006) L96–L98.
[33] S.J. Leach, H.A. Scheraga, Effect of light scattering on ultraviolet difference spectra, J. Am. Chem. Soc. 82 (1960) 4790–4792.
[34] K.O. Vanderwerf, C.A.J. Putman, B.G. Degrooth, F.B. Segerink, E.H. Schipper, N.F. Vanhulst, J. Greve, Compact stand-alone atomic-force microscope, Rev. Sci. Instrum. 64 (1993) 2892–2897.

[35] P.S. Chen, T.Y. Toribara, H. Warner, Microdetermination of phosphorus, Anal. Chem. 28 (1956) 1756–1758.
[36] R. Kayed, E. Head, J.L. Thompson, T.M. McIntire, S.C. Milton, C.W. Cotman, C.G. Glabe, Common structure of soluble amyloid oligomers implies common mechanism of pathogenesis, Science 300 (2003) 486–489.
[37] M. Zhu, J. Li, A.L. Fink, The association of alpha-synuclein with membranes affects bilayer structure, stability, and fibril formation, J. Biol. Chem. 278 (2003) 40186–40197.
[38] E. van den Brink-van der Laan, J.A. Killian, B. de Kruijff, Nonbilayer lipids affect peripheral and integral membrane proteins via changes in the lateral pressure profile, Biochim. Biophys. Acta 1666 (2004) 275–288.
[39] D. Marsh, Lateral pressure profile, spontaneous curvature frustration, and the incorporation and conformation of proteins in membranes, Biophys. J. 93 (2007) 3884–3899.
[40] J. Zimmerberg, M.M. Kozlov, How proteins produce cellular membrane curvature, Nat. Rev. Mol. Cell Biol. 7 (2006) 9–19.
[41] E.E. Kooijman, V. Chupin, N.L. Fuller, M.M. Kozlov, B. de Kruijff, K.N. Burger, P.R. Rand, Spontaneous curvature of phosphatidic acid and lysophosphatidic acid, Biochemistry 44 (2005) 2097–2102.
[42] J.H. Ipsen, O.G. Mouritsen, M. Bloom, Relationships between lipid membrane area, hydrophobic thickness, and acyl-chain orientational order. The effects of cholesterol, Biophys. J. 57 (1990) 405–412.
[43] B. Nuscher, F. Kamp, T. Mehnert, S. Odoy, C. Haass, P.J. Kahle, K. Beyer, Alpha-synuclein has a high affinity for packing defects in a bilayer membrane: a thermodynamics study, J. Biol. Chem. 279 (2004) 21966–21975.
[44] R. Lowe, D.L. Pountney, P.H. Jensen, W.P. Gai, N.H. Voelcker, Calcium(II) selectively induces alpha-synuclein annular oligomers via interaction with the C-terminal domain, Protein Sci. 13 (2004) 3245–3252.
[45] S. Tamamizu-Kato, M.G. Kosaraju, H. Kato, V. Raussens, J.M. Ruysschaert, V. Narayanaswami, Calcium-triggered membrane interaction of the alpha-synuclein acidic tail, Biochemistry 45 (2006) 10947–10956.
[46] I.F. Tsigelny, P. Bar-On, Y. Sharikov, L. Crews, M. Hashimoto, M.A. Miller, S.H. Keller, O. Platoshyn, J.X. Yuan, E. Masliah, Dynamics of alpha-synuclein aggregation and inhibition of pore-like oligomer development by beta-synuclein, FEBS J. 274 (2007) 1862–1877.
[47] H.J. Lee, C. Choi, S.J. Lee, Membrane-bound alpha-synuclein has a high aggregation propensity and the ability to seed the aggregation of the cytosolic form, J. Biol. Chem. 277 (2002) 671–678.
[48] S.D. Zakharov, J.D. Hulleman, E.A. Dutseva, Y.N. Antonenko, J.C. Rochet, W.A. Cramer, Helical alpha-synuclein forms highly conductive ion channels, Biochemistry 46 (2007) 14369–14379.
[49] W. Choi, S. Zibaee, R. Jakes, L.C. Serpell, B. Davletov, R.A. Crowther, M. Goedert, Mutation E46K increases phospholipid binding and assembly into filaments of human alpha-synuclein, FEBS Lett. 576 (2004) 363–368.
[50] P.H. Jensen, M.S. Nielsen, R. Jakes, C.G. Dotti, M. Goedert, Binding of alpha-synuclein to brain vesicles is abolished by familial Parkinson's disease mutation, J. Biol. Chem. 273 (1998) 26292–26294.
[51] D. Eliezer, E. Kutluay, R. Bussell Jr., G. Browne, Conformational properties of alpha-synuclein in its free and lipid-associated states, J. Mol. Biol. 307 (2001) 1061–1073.
[52] B.D. van Rooijen, M.M. Claessens, V. Subramaniam, Membrane binding of oligomeric alpha-synuclein depends on bilayer charge and packing, FEBS Lett. 582 (2008) 3788–3792.
[53] D. Allende, S.A. Simon, T.J. McIntosh, Melittin-induced bilayer leakage depends on lipid material properties: evidence for toroidal pores, Biophys. J. 88 (2005) 1828–1837.
[54] Y. Sokolov, J.A. Kozak, R. Kayed, A. Chanturiya, C. Glabe, J.E. Hall, Soluble amyloid oligomers increase bilayer conductance by altering dielectric structure, J. Gen. Physiol. 128 (2006) 637–647.
[55] G. van Meer, D.R. Voelker, G.W. Feigenson, Membrane lipids: where they are and how they behave, Nat. Rev. Mol. Cell Biol. 9 (2008) 112–124.
[56] S.J. Lee, Origins and effects of extracellular alpha-synuclein: implications in Parkinson's disease, J. Mol. Neurosci. 34 (2008) 17–22.
[57] W.W. Li, R. Yang, J.C. Guo, H.M. Ren, X.L. Zha, J.S. Cheng, D.F. Cai, Localization of alpha-synuclein to mitochondria within midbrain of mice, Neuroreport 18 (2007) 1543–1546.
[58] S. Shavali, H.M. Brown-Borg, M. Ebadi, J. Porter, Mitochondrial localization of alpha-synuclein protein in alpha-synuclein overexpressing cells, Neurosci. Lett. 439 (2008) 125–128.
[59] N.B. Cole, D. Dieuliis, P. Leo, D.C. Mitchell, R.L. Nussbaum, Mitochondrial translocation of alpha-synuclein is promoted by intracellular acidification, Exp. Cell Res. 314 (2008) 2076–2089.
[60] M. Ramakrishnan, P.H. Jensen, D. Marsh, Alpha-synuclein association with phosphatidylglycerol probed by lipid spin labels, Biochemistry 42 (2003) 12919–12926.
[61] C.C. Stichel, X.R. Zhu, V. Bader, B. Linnartz, S. Schmidt, H. Lubbert, Mono- and double-mutant mouse models of Parkinson's disease display severe mitochondrial damage, Hum. Mol. Genet. 16 (2007) 2377–2393.
[62] L. Devi, V. Raghavendran, B.M. Prabhu, N.G. Avadhani, H.K. Anandatheerthavarada, Mitochondrial import and accumulation of alpha-synuclein impair complex I in human dopaminergic neuronal cultures and Parkinson disease brain, J. Biol. Chem. 283 (2008) 9089–9100.
[63] M.S. Parihar, A. Parihar, M. Fujita, M. Hashimoto, P. Ghafourifar, Mitochondrial association of alpha-synuclein causes oxidative stress, Cell. Mol. Life Sci. 65 (2008) 1272–1284.